(will be inserted by the editor)

Volker D. Burkert

Nucleon Resonance Physics

Received: date / Accepted: date

Abstract Recent results of meson photo-production at the existing electron machines with polarized real photon beams and the measurement of polarization observables of the final state baryons have provided high precision data that led to the discovery of new excited nucleon and Δ states using multi-channel partial wave analyses procedures. The internal structure of several prominent excited states has been revealed employing meson electroproduction processes. On the theoretical front, lattice QCD is now predicting the baryon spectrum with very similar characteristics as the constituent quark model, and continuum QCD, such as is represented in the Dyson-Schwinger Equations approach and in light front relativistic quark models, describes the non-perturbative behavior of resonance excitations at photon virtuality of $Q^2 > 1.5 GeV^2$. In this talk I discuss the need to continue a vigorous program of nucleon spectroscopy and the study of the internal structure of excited states as a way to reveal the effective degrees of freedom underlying the excited states and their dependence on the distance scale probed.

Keywords Nucleon resonances, meson electroproduction, helicity amplitudes, quark models

1 Introduction

The excited states of the nucleon have been studied experimentally since the 1950's [1]. They contributed to the discovery of the quark model in 1964 by Gell-Mann and Zweig [2; 3], and were critical for the discovery of "color" degrees of freedom as introduced by Greenberg [4]. The quark structure of baryons resulted in the prediction of a wealth of excited states with underlying spin-flavor and orbital symmetry of $SU(6) \otimes O(3)$, and led to a broad experimental effort to search for these states. Most of the initially observed states were found with hadronic probes. However, of the many excited states predicted in the quark model, only a fraction have been observed to date. Search for the "missing" states and detailed studies of the resonance structure are now mostly carried out using electromagnetic probes and have been a major focus of hadron physics for the past decade [5]. A broad experimental effort is currently underway with measurements of exclusive meson photoproduction and electroproduction reactions, including many polarization observables. Precision data and the development of multi-channel partial wave analysis procedures have resulted in the discovery of several new excited states of the nucleon, which have been entered in the Review of Particle Physics [6].

A quantitative description of baryon spectroscopy and the structure of excited nucleons must eventually involve solving QCD for a complex strongly interacting multi-particle system. Recent advances

Volker D. Burkert Jefferson Laboratory

12000 Jefferson Avenue, Newport News, Virginia 23606

 $\begin{array}{l} {\rm Tel.:} +1~757~269~7540 \\ {\rm Fax:} +1~757~269~5800 \\ {\rm E\text{-}mail:} ~ {\rm burkert@jlab.org} \end{array}$

in Lattice QCD led to predictions of the nucleon spectrum in QCD with dynamical quarks [7], albeit with still large pion masses of 396 MeV. Lattice prediction can therefore only be taken as indicative of the quantum numbers of excited states and not of the masses of specific states. In parallel, the development of dynamical coupled channel models is being pursued with new vigor. The EBAC group at JLab has shown [8] that dynamical effects can result in significant mass shifts of the excited states. As a particularly striking result, a very large shift was found for the Roper resonance pole mass to 1365 MeV downward from its bare core mass of 1736 MeV. This result has clarified the longstanding puzzle of the incorrect mass ordering of $N(1440)\frac{1}{2}^+$ and $N(1535)\frac{1}{2}^-$ resonances in the constituent quark model. Developments on the phenomenological side go hand in hand with a world-wide experimental effort to produce high precision data in many different channel as a basis for a determination of the light-quark baryon resonance spectrum. On the example of experimental results from CLAS, the strong impact of precise meson photoproduction data is discussed. Several reviews have recently been published on this and related subjects [9; 10; 11; 12; 13].

It is interesting to point out recent findings that relate the observed baryon spectrum of different quark flavors with the baryon densities in the freeze out temperature in heavy ion collisions, which show evidence for missing baryons in the strangeness and the charm baryon sector [14; 15]. These data hint that an improved baryon model including further unobserved light quark baryons may resolve the current discrepancy between lattice QCD results and the results obtained using a baryon model that includes only states listed by the PDG. A complete accounting of excited baryon states of all flavors seems essential for a quantitative description of the occurrence of baryons in the evolution of the microsecond old universe.

Accounting for the complete excitation spectrum of the nucleon (protons and neutrons) and understanding the effective degrees of freedom is perhaps the most important and certainly the most challenging task of hadron physics. The experimental N* program currently focusses on the search for new excited states in the mass range from 2 GeV to 2.5 GeV using energy-tagged photon beams in the few GeV range, and the study of the internal structure of prominent resonances in meson electroproduction.

2 Establishing the N* Spectrum

The complex structure of the light-quark (u & d quarks) baryon excitation spectrum complicates the experimental search for individual states. As a result of the strong interaction, resonances are wide, often 200 MeV to 400 MeV, and are difficult to uniquely identify when only differential cross sections are measured. Most of the excited nucleon states listed in the Review of Particle Properties prior to 2012 have been observed in elastic pion scattering $\pi N \to \pi N$. However there are important limitations in the sensitivity to the higher mass nucleon states that may have small $\Gamma_{\pi N}$ decay widths. The extraction of resonance contributions then becomes exceedingly difficult in πN scattering. Estimates for alternative decay channels have been made in quark model calculations[16] for various channels. This has led to a major experimental effort at Jefferson Lab, ELSA, GRAAL, and MAMI to chart differential cross sections and polarization observables for a variety of meson photoproduction channels. At JLab with CLAS, several final states have been measured with high precision[17; 18; 19; 20; 21; 22; 23; 24; 25; 26] that are now employed in multi-channel analyses.

2.1 New states from open strangeness photoproduction

Here one focus has recently been on measurements of $\gamma p \to K^+ \Lambda$, using a polarized photon beam several polarization observables can be measured by analyzing the parity violating decay of the recoil $\Lambda \to p \pi^-$. It is well known that the energy-dependence of a partial-wave amplitude for one particular channel is influenced by other reaction channels due to unitarity constraints. To fully describe the energy-dependence of an amplitude one has to include other reaction channels in a coupled-channel approach. Such analyses have been developed by the Bonn-Gatchina group[27], at JLab[28], at Jülich[29] and other groups.

The data sets with the highest impact on resonance amplitudes in the mass range above 1.7 GeV have been kaon-hyperon production using a spin-polarized photon beam and where the polarization of

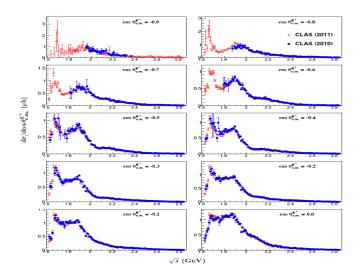


Fig. 1 Invariant mass dependence of the $\gamma p \to K^+ \Lambda$ differential cross section in the backward polar angle range. There are 3 structure visible that may indicate resonance excitations, at 1.7, 1.9, and 2.2 GeV. The blue full circles are based on the topology $K^+ p \pi^-$, the red open triangles are based on topology $K^+ p \pi^-$, which extended coverage towards lower W at backward angles and allows better access to the resonant structure near threshold.

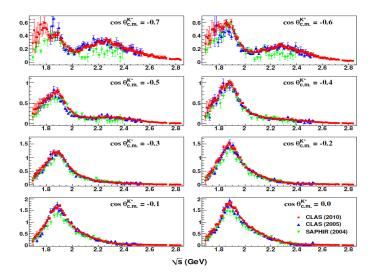


Fig. 2 Invariant mass dependence of the $\gamma p \to K^+ \Sigma^{\circ}$ differential cross section in the backward polar angle range.

the Λ or Σ° is also measured. The high precision cross section and polarization data [22; 23; 24; 25; 26] provide nearly full polar angle coverage and span the $K^{+}\Lambda$ invariant mass range from threshold to 2.9 GeV, hence covering the full nucleon resonance domain where new states might be discovered.

The backward angle $K^+\Lambda$ data in Fig.1 show clear resonance-like structures at 1.7 GeV and 1.9 GeV that are particularly prominent and well-separated from other structures at backward angles, while at more forward angles (not shown) t-channel processes become prominent and dominate the cross section. The broad enhancement at 2.2 GeV may also indicate resonant behavior although it

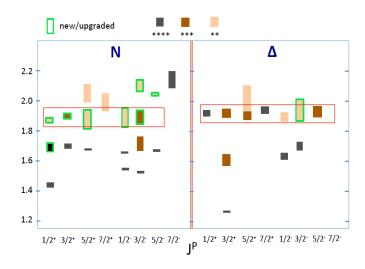


Fig. 3 Nucleon and Δ resonance spectrum below 2.2 GeV in RPP 2014 [6]. The new states and states with improved evidence observed in the recent Bonn-Gatchina multi-channel analysis are shown with the green frame. The red frames highlight the apparent mass degeneracy of five or six states with different spin and parity. The analysis includes all the $K^+\Lambda$ and $K^+\Sigma^{\circ}$ cross section and polarization data.

is less visible at more central angles with larger background contributions. The $K^+\Sigma$ channel also indicates significant resonant behavior as seen in Fig. 2. The peak structure at 1.9 GeV is present at all angles with a maximum strength near 90 degrees, consistent with the behavior of a $J^P = \frac{3}{2}^+$ p-wave. Other structures near 2.2 to 2.3 GeV are also visible. Still, only a full partial wave analysis can determine the underlying resonances, their masses and spin-parity. The task is somewhat easier for the $K\Lambda$ channel, as the iso-scalar nature of the Λ selects isospin- $\frac{1}{2}$ states to contribute to the $K\Lambda$ final state, while both isospin- $\frac{1}{2}$ and isospin- $\frac{3}{2}$ states can contribute to the $K\Sigma$ final state.

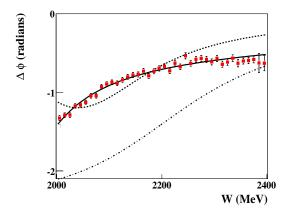


Fig. 4 Phase motion of the partial wave fit to the $\gamma p \to p \omega$ differential cross section and spin density matrix elements. 3 resonant states, the subthreshold resonance $N(1680)\frac{5}{2}^+$, $N(2190)\frac{7}{2}^-$, and the missing $N(2000)\frac{5}{2}^+$ are needed to fit the data (solid line). Fits without $N(2000)\frac{5}{2}^+$ (dashed-dotted line), or without $N(1680)\frac{5}{2}^+$ (dashed line) cannot reproduce the data.

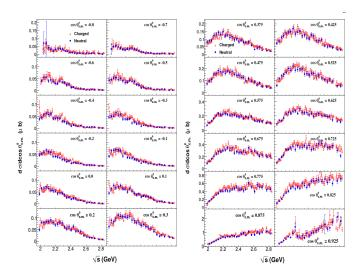


Fig. 5 Differential cross sections in a nearly full angular range for $\gamma p \to p \phi$ production.

These cross section data together with the Λ and Σ recoil polarization and polarization transfer data to the Λ and Σ had strong impact on the discovery of several new nucleon states. They also provided new evidence for several candidate states that had been observed previously but lacked confirmation as shown in Fig. 3. It is interesting to observe that five of the observed nucleon states have nearly degenerate masses near 1.9 GeV. Similarly, the new Δ state appears to complete a mass degenerate multiplet near 1.9 GeV as well. There is no obvious mechanism for this apparent degeneracy. Nonetheless, all new states may be accommodated within the symmetric constituent quark model based on $SU(6) \otimes O(3)$ symmetry group as far as quantum numbers are concerned. As discussed in section 1 for the case of the Roper resonance $N(1440)\frac{1}{2}^+$, the masses of all pure quark model states need to be corrected for dynamical coupled channel effects to compare them with observed resonances. The same applies to the recent Lattice QCD predictions [30] for the nucleon and Delta spectrum.

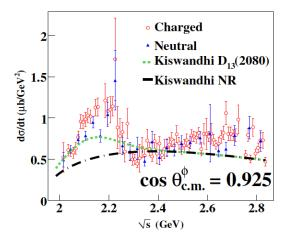


Fig. 6 Differential cross sections of $\gamma p \to p \phi$ production for the most forward angle bin. The two curves refer to fits without (dashed) and with (dotted) a known resonance at 2.08 GeV included.

2.2 Vectormeson photoproduction

In the mass range above 2.0 GeV resonances tend to decouple from simple final states like $N\pi$, $N\eta$, and $K\Lambda$. We have to consider more complex final states with multi-mesons or vector mesons, such as $N\omega$, $N\phi$, and $K^*\Sigma$. The study of such final states adds significant complexity as more amplitudes can contribute to spin-1 mesons photoproduction compared to pseudo-scalar meson production. As is the case for $N\eta$ production, the $N\omega$ channel is selective to isospin $\frac{1}{2}$ nucleon states only. CLAS has collected a tremendous amount of data in the $p\omega$ [20; 21] and $p\phi$ [31; 32] final states on differential cross sections and spin-density matrix elements that are now entering into the more complex multi-channel analyses such as Bonn-Gatchina [33]. The CLAS collaboration performed a single channel event-based analysis, whose results are shown in Fig. 4, and provide further evidence for the $N(2000)\frac{5}{2}^+$.

Photoproduction of ϕ mesons is also considered a potentially rich source of new excited nucleon states in the mass range above 2 GeV. Some lower mass states such as $N(1535)\frac{1}{2}^-$ may have significant $s\bar{s}$ components [34]. Such components may result in states coupling to $p\phi$ with significant strength above threshold. Differential cross sections and spin-density matrix elements have been measured for $\gamma p \to p\phi$ in a mass range up to nearly 3 GeV. In Fig. 5 structures are seen near 2.2 GeV in the forward most angle bins and at very backward angles for both decay channels $\phi \to K^+K^-$ and $\phi \to K_l^0K_s^0$, and with the exception of the smallest forward angle bin the structures are more prominent at backward angles. Only a multi-channel partial wave analysis will be able to pull out any significant resonance strength. Fig. 6 shows the differential cross section $d\sigma/dt$ of the most forward angle bin. A broad structure at 2.2 GeV is present, but does not show the typical Breit-Wigner behavior of a single resonance. It also does not fit the data in a larger angle range, which indicates that contributions other than genuine resonances may be significant. The forward and backward angle structures may also hint at the presence of dynamical effects possibly due to molecular contributions such as diquark-anti-triquark contributions [35], the strangeness equivalent to the recently observed hidden charm P_c^+ states.

Another process that has promise in the search for new excited baryon states, including those with isospin- $\frac{3}{3}$ is $\gamma p \to K^* \Sigma$ [33]. In distinction to the vector mesons discussed above, diffractive processes do not play a role in this channel, which then should allow better direct access to s-channel resonance production.

3 Structure of excited nucleons

Meson photoproduction has become an essential tool in the search for new excited baryons. The exploration of the internal structure of excited states and the effective degrees of freedom contributing to s-channel resonance excitation requires use of electron beams where the virtuality (Q^2) of the

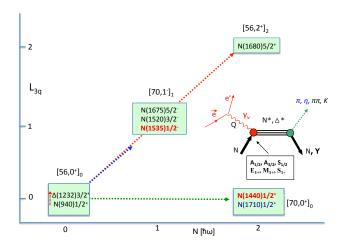


Fig. 7 Schematic of $SU(6) \otimes O(3)$ supermultiplets with excited states that have been explored in $ep \to e'\pi^+n$, $ep \to e'p'\pi^\circ$ and $ep \to e'p'\pi^+\pi^-$. The insert shows the helicity amplitudes and electromagnetic multipoles extracted from the data. Only the ones highlighted in red are discussed here.

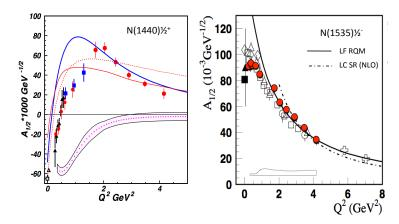


Fig. 8 Left panel: The transverse helicity amplitudes $A_{1/2}$ for the Roper resonance $N(1440)\frac{1}{2}^+$. Data are from CLAS compared to two LF RQM with fixed quark masses (dashed) and with running quark mass (solid red), and with projections from the DSE/QCD approach. The magenta dotted line with error band indicates non 3-quark contributions obtained from a the difference of the DSE curve and the CLAS data. The right panel shows the same amplitude for the $N(1535)\frac{1}{2}^-$ compared to LF RQM calculations (solid line) and QCD computation within the LC Sum Rule approach.

exchanged photon can be varied to probe the spatial structure (Fig. 7). Electroproduction of final states with pseudoscalar mesons (e.g. $N\pi$, $p\eta$, $K\Lambda$) have been employed with CLAS, leading to new insights into the scale dependence of effective degrees of freedom, e.g. meson-baryon, constituent quark, and dressed quark contributions. Several excited states, shown in Fig. 7 assigned to their primary $SU(6)\otimes O(3)$ supermultiplets have been studied. The $N\Delta(1232)\frac{3}{2}^+$ transition is now well measured in a large range of Q^2 [36; 37; 38; 40]. Two of the prominent higher mass states, the Roper resonance $N(1440)\frac{1}{2}^+$ and $N(1535)\frac{1}{2}^-$ are shown in Fig. 8 as representative examples [39; 40] from a wide program at JLab [41; 42; 43; 44; 45; 46]. For these two states advanced relativistic quark model calculations [47] and QCD calculations Dyson-Schwinger Equation [48] and Light Cone sum rule [49] have recently become available, for the first time employing QCD-based modeling of the excitation of the quark core. There is agreement with the data at $Q^2 > 1.5 \text{ GeV}^2$. The calculations deviate significantly from the data at lower Q^2 , which indicates significant non quark core effects. For the Roper resonance such contributions have been described successfully in dynamical meson-baryon models [50] and in effective field theory [51].

Knowledge of the helicity amplitudes in a large Q^2 allows for the determination of the transition charge densities on the light cone in transverse impact parameter space (b_x, b_y) [52]. Figure 9 shows the comparison of $N(1440)\frac{1}{2}^+$ and $N(1535)\frac{1}{2}^-$. There are clear differences in the charge transition densities between the two states. The Roper state has a softer positive core and a wider negative outer cloud than N(1535) and develops a larger shift in b_y when the proton is polarized along the b_x axis.

4 Conclusions and Outlook

Over the past five years eight baryon states in the mass range from 1.85 to 2.15 GeV have been either discovered or evidence for the existence of states has been significantly strengthened. To a large degree this is the result of adding very precise photoproduction data in open strangeness channels to the data base that is included in multi-channel partial wave analyses, especially the Bonn-Gatchina PWA. The possibility to measure polarization observables in these processes has been critical [53]. In the mass range above 2 GeV more complex processes such as vector mesons or $\Delta\pi$ may have sensitivity to states with higher masses but require more complex analyses techniques to be brought to bear. Precision data in such channels have been available for a few years but remain to be fully incorporated in multi-channel partial wave analyses processes. The light-quark baryon spectrum is likely also populated with hybrid

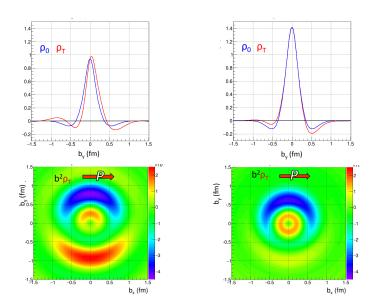


Fig. 9 Left panels: N(1440), top: projection of charge densities on b_y , bottom: transition charge densities when the proton is spin polarized along b_x . Right panels: same for N(1535). Note that the densities are scaled with b^2 to emphasize the outer wings. Color code:negative charge is blue, positive charge is red. Note that all scales are the same.

excitations [7] where the gluonic admixtures to the wave function are dominating the excitation. These states appear with the same quantum numbers as ordinary quark excitations, and can only be isolated from ordinary states due to the Q^2 dependence of their helicity amplitudes [54], which is expected to be quite different from ordinary quark excitations. This requires new electroproduction data especially at low Q^2 [55] with different final states and at masses above 2 GeV.

Despite the very significant progress made in recent years to further establish the light-quark baryon spectrum and explore the internal structure of excited states, much remains to be done. A vast amount of precision data already collected needs to be included in the multi-channel analysis frameworks, and polarization data are still to be analyzed [53]. There are approved proposals to study resonance excitations at much higher Q^2 and with higher precision at Jefferson Lab with CLAS12 [56] that may reveal the transition to the bare quark core contributions at short distances.

5 Acknowledgment

I like to thank Inna Aznauryan and Viktor Mokeev for numerous discussions on the subjects discussed in this presentation. This work was supported by the US Department of Energy under contract No. DE-AC05-06OR23177.

References

- 1. H. L. Anderson, E. Fermi, E. A. Long and D. E. Nagle (1952) Phys. Rev. 85, 936.
- M. Gell-Mann, Phys. Lett. 8, 214 (1964).
- G. Zweig, CERN Reports, TH 401 and 412 (1964).
- O. W. Greenberg, Phys. Rev. Lett. 13, 598 (1964); arXiv:0803.0992 [physics.hist-ph].
 V. D. Burkert and T. S. H. Lee Int. J. Mod. Phys. E 13, 1035 (2004).
- 6. K. A. Olive et al. [Particle Data Group], Chin. Phys. C 38, 090001 (2014).
- 7. J. J. Dudek and R. G. Edwards, Phys. Rev. D 85, 054016 (2012)
- N. Suzuki et al., Phys. Rev. Lett. 104, 042302 (2010)
- 9. E. Klempt and J. M. Richard, Rev. Mod. Phys. 82, 1095 (2010)
- 10. L. Tiator, D. Drechsel, S. S. Kamalov and M. Vanderhaeghen, Eur. Phys. J. ST 198, 141 (2011). 11. I. G. Aznauryan and V. D. Burkert, Prog. Part. Nucl. Phys. 67, 1 (2012)

12. I. G. Aznauryan et al., Int. J. Mod. Phys. E 22, 1330015 (2013) 13. V. Crede and W. Roberts, Rept. Prog. Phys. **76**, 076301 (2013) 14. A. Bazavov et al., Phys. Rev. Lett. 113, no. 7, 072001 (2014) [arXiv:1404.6511 [hep-lat]]. 15. A. Bazavov et al., Phys. Lett. B 737, 210 (2014) [arXiv:1404.4043 [hep-lat]]. 16. S. Capstick and W. Roberts, Phys. Rev. D 49, 4570 (1994)
 17. M. Dugger et al., Phys. Rev. Lett. 96, 062001 (2006) [Phys. Rev. Lett. 96, 169905 (2006)]
 18. M. Dugger et al. [CLAS Collaboration], Phys. Rev. C 79, 065206 (2009) doi:10.1103/PhysRevC.79.065206 19. M. Williams *et al.* [CLAS Collaboration], Phys. Rev. C **80**, 045213 (2009) 20. M. Williams *et al.* [CLAS Collaboration], Phys. Rev. C **80**, 065209 (2009) 20. M. Williams *et al.* [CLAS Collaboration], Phys. Rev. C **80**, 065209 (2009) 21. M. Williams *et al.* [CLAS Collaboration], Phys. Rev. C **80**, 065208 (2009) R. K. Bradford *et al.* [CLAS Collaboration], Phys. Rev. C **75**, 035205 (2007)
 R. Bradford *et al.* [CLAS Collaboration], Phys. Rev. C **73**, 035202 (2006) 24. M. E. McCracken et al. [CLAS Collaboration], Phys. Rev. C 81, 025201 (2010) 25. B. Dey et al. [CLAS Collaboration], Phys. Rev. C 82, 025202 (2010) 26. J. W. C. McNabb et al. [CLAS Collaboration], Phys. Rev. C 69, 042201 (2004) 27. A. Anisovich, R. Beck, E. Klempt, V. Nikonov, A. Sarantsev and U. Thoma, Eur. Phys. J. A **48**, 15 (2012) 28. B. Julia-Diaz, T.-S. H. Lee, A. Matsuyama and T. Sato, Phys. Rev. C **76**, 065201 (2007) 29. D. Rönchen et al., Eur. Phys. J. A 50, no. 6, 101 (2014) B. Ronchen et al., Edit. Phys. 3. A 30, no. 6, 101 (2014)
 R. G. Edwards, J. J. Dudek, D. G. Richards and S. J. Wallace, Phys. Rev. D 84, 074508 (2011)
 H. Seraydaryan et al. [CLAS Collaboration], Phys. Rev. C 89, no. 5, 055206 (2014)
 B. Dey et al. [CLAS Collaboration], Phys. Rev. C 89, no. 5, 055208 (2014) 33. A. Sarantsev, talk at this workshop
34. B. C. Liu and B. S. Zou, Phys. Rev. Lett. **96**, 042002 (2006) 35. R. F. Lebed, Phys. Rev. D 92, no. 11, 114030 (2015) 36. K. Joo et al. [CLAS Collaboration], Phys. Rev. Lett. 88, 122001 (2002) 37. M. Ungaro et al. [CLAS Collaboration], Phys. Rev. Lett. 97, 112003 (2006) 38. V. V. Frolov *et al.*, Phys. Rev. Lett. **82**, 45 (1999) 39. I. G. Aznauryan *et al.* [CLAS Collaboration], Phys. Rev. C **78**, 045209 (2008) 40. I. G. Aznauryan *et al.* [CLAS Collaboration], Phys. Rev. C **80**, 055203 (2009) 41. V. I. Mokeev *et al.* [CLAS Collaboration], Phys. Rev. C **86**, 035203 (2012) 42. H. Denizli *et al.* [CLAS Collaboration], Phys. Rev. C **76**, 015204 (2007) 43. C. S. Armstrong *et al.* [Jefferson Lab E94014 Collaboration], Phys. Rev. D **60**, 052004 (1999) 44. H. Egiyan *et al.* [CLAS Collaboration], Phys. Rev. C **73**, 025204 (2006) 45. K. Park *et al.* [CLAS Collaboration], Phys. Rev. C **77**, 045208 (2008) 46. K. Park et al. [CLAS Collaboration], Phys. Rev. C **91**, 045203 (2015) 47. I. G. Aznauryan and V. D. Burkert, Phys. Rev. C **92**, no. 3, 035211 (2015) 48. J. Segovia et al., Phys. Rev. Lett. **115**, no. 17, 171801 (2015) 49. I. V. Anikin, V. M. Braun and N. Offen, Phys. Rev. D 92, no. 1, 014018 (2015) 50. I. T. Obukhovsky et al., Phys. Rev. D 84, 014004 (2011) 51. T. Bauer, S. Scherer and L. Tiator, Phys. Rev. C 90, no. 1, 015201 (2014) 52. L. Tiator and M. Vanderhaeghen, Phys. Lett. B 672, 344 (2009)

55. L. Lanza, talk at this workshop; A. D' Angelo et al., Jefferson Lab Letter of Intent LOI12-15-004 (2015).

53. E. Pasyuk, talk at this workshop.

54. Z. p. Li, V. Burkert and Z. j. Li, Phys. Rev. D 46, 70 (1992).

56. R. Gothe, D. Carman, V. Mokeev, K. Park, talks at this workshop.